Contents List available at VOLKSON PRESS

New Materials and Intelligent Manufacturing (NMIM)

DOI : http://doi.org/10.26480/icnmim.01.2018. 287.289

Journal Homepage : https://topicsonchemeng.org.my/

ISBN: 978-1-948012-12-6

PHOTOTHERMAL EVALUATION OF CUS@CU$_2$S NANOPARTICLES PREPARED BY HYDROTHERMAL SYNTHESIS

Tian Lining, Qing Tizhi, Wang Duoying, Zhao Jinghan, Wang Chen and Zhang Yu*

Jilin Institute of Chemical Technology Jilin City, China
Corresponding author email: zhang99yu@hotmail.com

ARTICLE DETAILS

Article History:

Received 26 June 2018
Accepted 2 July 2018
Available online 1 August 2018

ABSTRACT

In order to evaluate the photothermal effect of CuS@Cu$_2$S nanoparticles, photothermal temperature curves and images were observed by an infrared camera, and photothermal efficiency was calculated by linear fitting. The results show that CuS@Cu$_2$S nanoparticles have higher temperature increase under 808 nm laser irradiation, which can be proved by near-infrared (NIR) thermal images. Moreover, high photothermal conversion efficiency of CuS@Cu$_2$S can be adjusted by the content of Cu$_2$S.

KEYWORDS

Photothermal, CuS@Cu$_2$S, Nanoparticles, Linear fitting.

1. INTRODUCTION

As potential semiconductors, copper sulphide (CuS) nanoparticles have been paid extensive attentions [1,2]. CuS is one of the most important p-type semiconductor materials, which has been fabricated by a variety of morphologies such as nanoparticles, nanowires, nanoplates, nanorods, nanotubes, ball-flower, hollow sphere and hollow cages by different methods [3-6]. CuS nanoparticles show excellent performance in photocatalytic degradation of dyes, gas sensing, solar cell, lithium ion batteries, etc [7-11].

Cuprous sulfide (Cu$_2$S) is also a p-type semiconductor, which prohibits a great potential in energy and catalysis field, such as solar cells, catalysis, solar energy conversion, biosensors, efficient photo catalyst and a certain optoelectronics equipment [12-16].

Recently, CuS@Cu$_2$S have attracted more and more attention due to their unique structure and excellent properties in physical and chemical, which have been successfully used to degrade methyl violet, rhodamine B, methyl orange and methylene blue by UV–vis spectrum analyzer [17, 18]. In this work, CuS@Cu$_2$S nanoparticles were synthesized by hydrothermal method, and the photothermal effects of CuS@Cu$_2$S nanoparticles were investigated.

2. EXPERIMENTAL

2.1 Materials and Synthesis

Copper chloride ($CuCl_2{\cdot}2H_2O$) and sodium sulphide ($Na_2S{\cdot}9H_2O$) were obtained from Tianjin Damao Chemical Regent Co., Ltd. Polyvinylpyrrolidone (PVP-K30) was obtained from Beijing Yili Chemical Co., Ltd. Sodium hydroxide (NaOH) and hydrazine anhydrous solution ($N_2H_4{\cdot}H_2O$) were purchased from Tianjin Damao Chemical Regent Co., Ltd. Sodium borohydride ($NaBH_4$) was purchased from Sinopharm Chemical Reagent Co., Ltd.

CuS@Cu$_2$S nanoparticles were prepared by a previously related method with slight modification. Firstly, 120 μL $CuCl_2$ solution (0.5 M) was added to 30 mL deionized (DI) water including 0.25 g PVP-K30 under slight stirring at 25°C. Then, 30 mL NaOH solution (pH = 9.0) and 6.5 μL $N_2H_4{\cdot}H_2O$ (50%) was injected to form Cu$_2$O spheres. After 5 min, 220 μL Na_2S aqueous solution (320 mg mL^{-1}) was added to the solution. Then, the mixture was heated for 2 h at 60 °C and collected by centrifugal method at 14000 rpm for 10 min with four times DI water washed. Finally, the CuS nanoparticles were suspended in 20 mL ethanol, followed by the addition of 0.15 g PVP-K30. Then, different $NaBH_4$ (3 mM) was added and stirred for 1 h. The CuS@Cu$_2$S nanoparticles were washed and dispersed in 20 mL water.

2.2 Photothermal measurement

To evaluate the photothermal effect of CuS@Cu$_2$S nanoparticles in solution, 180 μL solutions with different CuS@Cu$_2$S concentrations and Cu$_2$S volumes were deposited into centrifuge tube. Then, the tubes were irradiated by an 808 nm laser at different power density (0.5, 0.8 and 1.0 W cm^{-2}) with the increasing time. All the temperatures and images were achieved by a multi-wavelength laser device (fabricated by Jilin Institute of Chemical Technology) containing both high-power laser and infrared thermal imaging camera.

2.3 Linear fitting and calculation

According to the eq1, the photothermal conversion efficiency (η) of CuS@Cu$_2$S was calculated by the temperature cooling results [19].

$$\eta = [hs(T_{max} - T_{surr}) - Q_{dis}]/[I - (1 - 10^{-A_{808}})] \quad \text{eq1}$$

T_{max} —— equilibrium temperature;
T_{surr} —— ambient temperature of the surroundings;
Q_{dis} ——heat loss from light absorbed by the container (~ 0 mW);
I —— incident laser power (0.5 W cm^{-2});
A_{808} —— the absorbance of samples at 808 nm;
h —— heat transfer coefficient;
s —— surface area of the container;
h_s —— calculated using the following eq2 [19]:

$$\tau_s = m_D c_D / h_s \quad \text{eq2}$$

τ_s —— sample system time constant;
m_D —— mass of the solvent;
c_D —— heat capacity of the solvent.

3. RESULT AND DISCUSSION

3.1 Evaluation of CuS@Cu_2S photothermal behavior

Figure 1A displays the temperature elevation of CuS@Cu_2S, CuS and DI water under 808 nm laser irradiation. With time goes on, CuS@Cu_2S aqueous solution (100 ppm) increases to a higher temperature of 67.3 °C (808 nm, 0.5 W cm^{-2}, 7 min). However, CuS and pure water only increase to 32.0 and 23.2 °C, respectively. Moreover, after three cycles of heating and cooling, the photothermal effect of CuS@Cu_2S still remains good (Figure 1B). Figure 1C, D exhibits that both CuS@Cu_2S concentration and laser power density are proportional to the temperature increment, respectively. All the related results of temperature increasing can be proved by the images of the NIR thermal images (Figure 2).

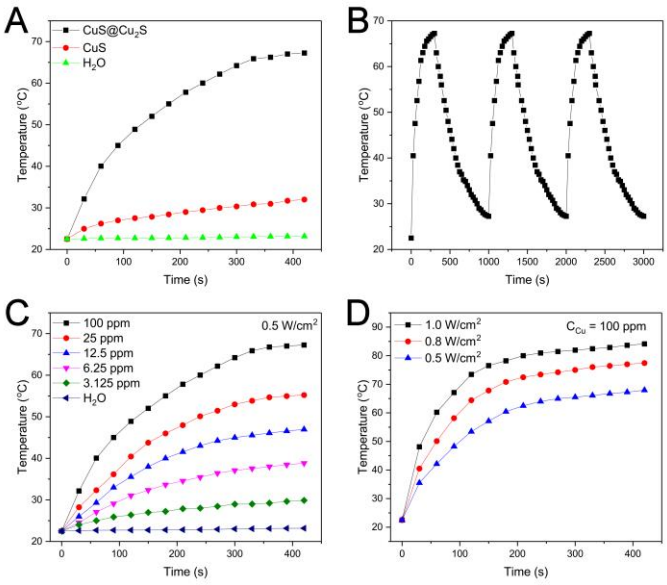

Figure 1: (A) Photothermal temperature curves of CuS@Cu_2S, CuS, and DI water; (B) The photothermal conversion cycling test of CuS@Cu_2S aqueous solution; (C) Photothermal conversion characterizations of CuS@Cu_2S aqueous solution with different concentrations under 808 nm laser irradiation (0.5 W cm^{-2}, 420 s); (D) Photothermal conversion characterizations of CuS@Cu_2S aqueous solution under different power density of 808 nm laser irradiation (C_{Cu} = 100 ppm, 420 s).

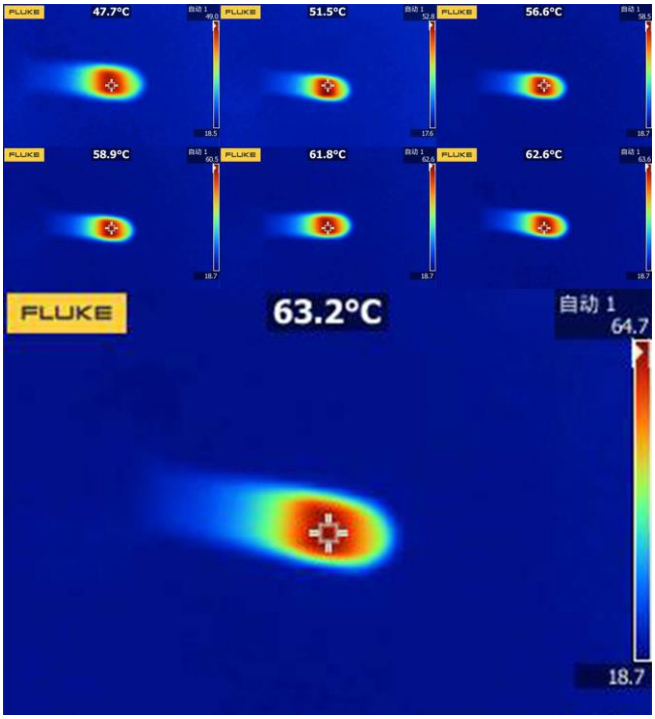

Figure 2: NIR thermal images CuS@Cu_2S

3.2 Photothermal conversion efficiency of CuS@Cu_2S

The temperatures increasing and cooling of specimens with different Cu_2S was also detected. Figure 3A shows that the temperature increases with the increasing concentration of Cu_2S. Furthermore, the highest (27.9) was obtained at the Cu_2S volume of 10 mL, which is similar to the temperature increasing (Figure 3B). These photothermal conversion efficiency results were calculated by the linear fitting, indicating the data of η value are repeatability (Figure 3C-H) [20].

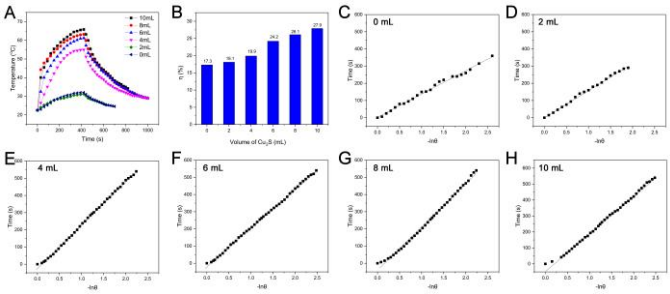

Figure 3: (A) Temperature increasing and cooling curves of CuS@Cu_2S; (B) Photothermal conversion efficiency (η) of CuS@Cu_2S; (C-H) Linear time data gained from A.

4. CONCLUSIONS

In summary, we have successfully prepared the CuS@Cu_2S nanoparticles by using hydrothermal synthesis. The excellent photothermal effect of CuS@Cu_2S specimens were achieved with increasing concentration and high photothermal conversion efficiency were obtained with high Cu_2S volume. In addition, good linear fitting results were gained by formula calculation, illustrating the stability of the photothermal effect.

ACKNOWLEDGE

We are grateful to Technological innovation development plan project of Jilin city (20161205) and Major technological project of Jilin Institute of Chemical Technology (2015018) for financial support.

REFERENCES

[1] Tian, Q., Hu, J., Zhu, Y. 2013. Sub-10nm Fe_3O_4@$Cu_{2-x}S$ Core-Shell Nanoparticles for Dual-Modal Imaging and Photothermal Therapy. J. Am. Chem. Soc, 135, 8571-8577.

[2] Tian, Q.W., Tang, M.H., Sun, Y.G. 2011. Hydrophilic Flower-Like CuS Superstructures as an Efficient 980 nm Laser-Driven Photothermal Agent for Ablation of Cancer Cells. Adv. Mater, 23, 3542-3547.

[3] Zha, Z.B., Wang, S.M., Zhang, S.H. 2013. Targeted Delivery of CuS Nanoparticles Through Ultrasound Image-Guided Microbubble Destruction for Efficient Photothermal Therapy. Nanoscale, 5, 3216-3219.

[4] Zhou, M., Zhang, R., Huang, M. 2010. A Chelator-Free Multifunctional [^{64}Cu] CuS Nanoparticle Platform for Simultaneous Micro-PET/CT Imaging and Photothermal Ablation Therapy. J. Am. Chem. Soc, 132, 15351-15358.

[5] Dai, Y., Xiao, H., Liu, J. 2013. In Vivo Multimodality Imaging and Cancer Therapy by Near-Infrared Light-Triggered trans-Platinum Pro-Drug-Conjugated Upconverison Nanoparticles. J. Am.Chem. Soc, 135, 18920-18929.

[6] Zeng, S., Yi, Z., Lu, W. 2014. Simultaneous Realization of Phase/Size Manipulation, Upconversion Luminescence Enhancement, and Blood Vessel Imaging in Multifunctional Nanoprobes Through Transition Metal Mn^{2+} Doping. Adv. Funct. Mater, 24, 4051-4059.

[7] Ostrowski, A.D., Chan, E.M., Gargas, D.J. 2012. Controlled Synthesis and Single-Particle Imaging of Bright, Sub-10 nm Lanthanide-Doped Upconverting Nanocrystals. ACS Nano, 6, 2686-2692.

[8] Zheng, W., Huang, P., Tu, D. 2015. Lanthanide-Doped Upconversion Nano-Bioprobes: Electronic Structures, Optical Properties, and Biodetection. Chem. Soc. Rev, 44, 1379-1415.

[9] Liu, X., Yan, C.H., Capobianco, J.A. 2015. Photon Upconversion Nanomaterials. Chem. Soc. Rev, 44, 1299-1301.

[10] Li, Y., Tang, J., Pan, D.X. 2016. A Versatile Imaging and Therapeutic Platform Based on Dual-Band Luminescent Lanthanide Nanoparticles toward Tumor Metastasis Inhibition. ACS Nano, 10, 2766-2773.

[11] Zhou, J., Liu, Q., Feng, W. 2015. Upconversion Luminescent Materials: Advances and Applications. Chem. Rev, 115, 395-465.

[12] Liu, Z., Ran, X., Liu, J. 2016. Non-Toxic Lead Sulfide Nanodots as Efficient Contrast Agents for Visualizing Gastro-intestinal Tract. Biomaterials, 100, 17-26.

[13] Stouwdam, J.W., van Veggel, F. 2004. Improvement in the Luminescence Properties and Processability of LaF_3/Ln and $LaPO_4$/Ln Nanoparticles by Surface Modification. Langmuir, 20, 11763-11771.

[14] Wang, S., Li, X., Chen, Y. 2015. A Facile One-Pot Synthesis of a Two-Dimensional MoS_2/Bi_2S_3 Composite Theranostic Nanosystem for Multi-Modality Tumor Imaging and Therapy. Adv. Mater, 27, 2775-2782.

[15] Kim, J., Piao, Y., Hyeon, T. 2009. Multifunctional Nanostructured Materials for Multimodal Imaging, and Simultaneous Imaging and Therapy. Chem. Soc. Rev, 38, 372-390.

[16] Liu, B., Li, C., Xing, B. 2016. Nanocomposites for Upconversion Imaging and Combined Photothermal/Photodynamic Therapy with Enhanced Antitumor Efficacy. J. Mater. Chem. B, 4, 4884-4894.

[17] Bardhan, R., Chen, W., Perez-Torres, C. 2009. Nanoshells with Targeted Simultaneous Enhancement of Magnetic and Optical Imaging and Photothermal Therapeutic Response. Adv. Funct. Mater, 19, 3901-3909.

[18] Hu, M., Chen, J.Y., Li, Z.Y. 2006. Gold Nanostructures: Engineering Their Plasmonic Properties for Biomedical Applications. Chem. Soc. Rev, 35, 1084-1094.

[19] Zhang, C., Bu, W., Ni, D. 2016. A Polyoxometalate Cluster Paradigm with Self-Adaptive Electronic Structure for Acidity/Reducibility-Specific Photothermal Conversion. J. Am.Chem. Soc, 138, 8156-8164.

[20] Elsayed, J. 2017. Bio-Chemical Biomarkers In Algae Scenedesmus Obliquus Exposed To Heavy Metals Cd, Cu And Zn. Acta Chemica Malaysia, 1 (1), 16-20.